



Redefinition of angastonite, $\text{CaMgAl}_2(\text{PO}_4)_2(\text{OH})_4 \cdot 7\text{H}_2\text{O}$, as an amorphous mineral

Ian Edward Grey¹, Peter Elliott^{2,3}, William Gus Mumme¹, Colin M. MacRae¹, Anthony R. Kampf⁴, and
Stuart J. Mills⁵

¹CSIRO Mineral Resources, Private Bag 10, Clayton South 3169, Victoria, Australia

²Department of Earth Sciences, School of Physical Sciences, The University of Adelaide,
Adelaide 5005, South Australia, Australia

³South Australian Museum, North Terrace, Adelaide 5000, South Australia, Australia

⁴Mineral Sciences Department, Natural History Museum of Los Angeles County,
900 Exposition Boulevard, Los Angeles, CA 90007, USA

⁵Geosciences, Museums Victoria, GPO Box 666, Melbourne 3001, Victoria, Australia

Correspondence: Ian Edward Grey (ian.grey@csiro.au)

Received: 28 January 2022 – Revised: 18 March 2022 – Accepted: 21 March 2022 – Published: 7 April 2022

Abstract. A reinvestigation of the type angastonite specimen from the Penrice marble quarry, South Australia, shows that the published powder X-ray diffraction pattern for the mineral corresponds to a mixture of crystalline phases plus an amorphous phase. The published formula for the mineral, $\text{CaMgAl}_2(\text{PO}_4)_2(\text{OH})_4 \cdot 7\text{H}_2\text{O}$, has been found to correspond to the amorphous phase. A proposal for the redefinition of angastonite as an amorphous phase has been approved by the IMA CNMNC. Amorphous angastonite is isotropic with an index of refraction in the range 1.33 to 1.40 and a measured density of $1.57(2) \text{ g cm}^{-3}$. It is formed from incongruent leaching of minyulite in circulating Mg- and Ca-bearing solutions. The amorphous phase undergoes local recrystallisation to form penriceite and two other new crandallite-derivative layer phases. A cluster model for the local structure in the amorphous mineral is proposed based on crandallite-type segments. A brief review of amorphous minerals is given.

1 Introduction

Mills et al. (2008) described a new phosphate mineral from the Penrice marble quarry, South Australia, that they named angastonite after Angaston, a town near to the quarry. From electron microprobe analyses they gave the formula as $\text{CaMgAl}_2(\text{PO}_4)_2(\text{OH})_4 \cdot 7\text{H}_2\text{O}$. Their paper shows a scanning electron microscope (SEM) image of angastonite in Museums Victoria specimen M45575 that they described as “contorted platelets of angastonite that have replaced a pre-existing phosphate” (their Fig. 5). They also show an SEM image of hexagonal-shaped ultrathin (1–2 μm) platelets in the Museums Victoria type specimen M50494 (their Fig. 4) that they considered to be better-crystallised forms of the mineral. They indexed the powder X-ray diffraction (PXRD) pattern using a triclinic cell but were not able to solve the crystal structure.

In a study of secondary phosphate minerals from the angastonite type locality, we collected single-crystal synchrotron data on a platelet with the same appearance as those shown in Fig. 4 of Mills et al. (2008) and solved the structure. It was found to be the fluoride analogue, $[\text{Mg}(\text{H}_2\text{O})_6][\text{Na}(\text{H}_2\text{O})_2\text{Al}_3(\text{PO}_4)_2\text{F}_6] \cdot \text{H}_2\text{O}$ of aldermanite (Elliott et al., 2021), and a proposal for the mineral and its name, penriceite, has been approved by the IMA Commission on New Minerals, Nomenclature and Classification (IMA2021-068; Elliott et al., 2022). The positions and relative intensities of the PXRD lines for this mineral were found to match those of the strongest lines in the reported PXRD pattern for angastonite (Mills et al., 2008). Their pattern contains, in addition, numerous other lines, the strongest being at $d = 11.05$ and $d = 10.20 \text{ \AA}$. From PXRD studies on museum specimens from the Penrice quarry and the nearby Tom’s

phosphate quarry, we have isolated fragments that have either the 11.05 or the 10.2 Å peak as the strongest peak in the PXRD pattern and have determined the structures corresponding to these two phases. They correspond to derivative structures of crandallite, $\text{CaAl}_3(\text{PO}_4)(\text{PO}_3\text{OH})(\text{OH})_6$, with expanded layer separations of 11.05 and 10.2 Å due to the incorporation of hydrated $\text{Mg}(\text{H}_2\text{O})_6^{2+}$ octahedra and H_2O molecules in place of Ca in the interlayer region. As they have not yet been approved as new minerals, we refer to them here as the 10 and 11 Å phases. Thus, the PXRD pattern reported for angastonite comprises contributions from three new crystalline phosphate minerals. In addition, the PXRD has broad humps located at $d \approx 4.1$ and $d \approx 3.0$ Å corresponding to an amorphous-phase contribution.

Scanning electron microscope (SEM) images of type angastonite show, in addition to the phases with platy morphology (penriceite, 11 and 10 Å phases) and minyulite, the presence of anhedral grains, which have the same analysis as reported for angastonite. The translucent, glassy anhedral grains were checked by single-grain X-ray diffraction (XRD) and were found to be amorphous. A submission to the IMA CNMNC for a redefinition of angastonite as an amorphous phase (proposal 21-J) has been approved (Miyawaki et al., 2022), and we report here the characterisation of amorphous angastonite and its role in the paragenesis of the crandallite-derivative phases.

2 Occurrence and paragenesis

In the angastonite type specimen, Museums Victoria specimen M45575, amorphous angastonite is present as rounded grains, underlying strongly etched minyulite laths and associated with $\sim 1 \mu\text{m}$ thick platy minerals as shown in Fig. 1. Other associated minerals include wavellite, crandallite, iangreyite, quartz and goethite. Angastonite is formed from incongruent dissolution of minyulite in near-neutral Mg- and Ca-bearing solutions (Grey et al., 2022). Minyulite, formula $\text{KAl}_2\text{F}(\text{PO}_4)_2 \cdot 4\text{H}_2\text{O}$, a common mineral in phosphate deposits of the Kapunda–Angaston region of South Australia (Elliott et al., 2013), is stable at relatively low pH ($\text{pH} \approx 3$) under conditions of ready supply of K and F (Tatur, 1987). With decreasing acidity of the circulating meteoric solutions, minyulite breaks down to an amorphous phase (Haseman et al., 1950). Figure 2 shows minyulite crystals in a specimen from Tom’s quarry that have undergone surface alteration to angastonite.

3 Description and experimental procedures

3.1 Appearance and properties

Angastonite grains are anhedral with a translucent, glassy appearance and conchoidal fracture. Angastonite coatings on minyulite are often found extending over several millime-

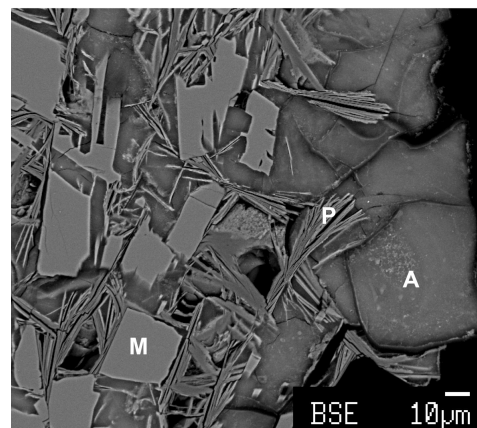


Figure 1. Back-scattered electron image of angastonite type specimen M45575. M denotes minyulite; P denotes penriceite; A denotes amorphous angastonite.



Figure 2. Amorphous angastonite coating minyulite crystals from Tom’s quarry. The field of view is 4 mm across.

tres in hand specimens. The colour is off-white to beige, and the streak is white. Measurement of the density of angastonite in the type specimen gave an anomalously low value of 1.15 g cm^{-3} , most likely due to trapped air. The density of angastonite in the Tom’s quarry specimen, measured by flotation in a mixture of methylene iodide and toluene, is $1.57(2) \text{ g cm}^{-3}$. Initially, attempts were made to measure the index of refraction of angastonite using Cargille immersion liquids; however, it was found to be lower than the lowest available liquid with $n = 1.40$. Subsequent measurements using mixtures of glycerol and water with indices of refraction determined with a refractometer gave $n = 1.33$ to $n = 1.34$ for angastonite in the type specimen and $n = 1.39$ to $n = 1.40$ for angastonite in the Tom’s quarry specimen. Application of the Gladstone–Dale relationship (Mandarino, 1981) with $n = 1.395$, a density of 1.57 g cm^{-3} and the empirical formula for the Tom’s quarry specimen gives a compatibility index of -0.035 (EXCELLENT).

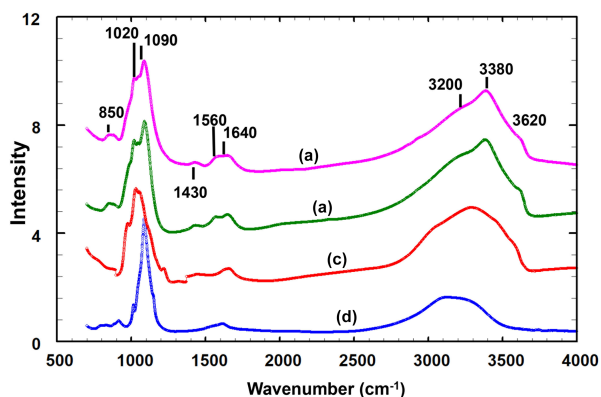


Figure 3. Infrared spectra for the (a) amorphous phase in the Penrice type locality specimen, (b) amorphous phase in angastonite type specimen M45575, (c) penriceite from the type locality and (d) minyulite associated with the amorphous phase in the type specimen.

3.2 Infrared spectroscopy

Infrared spectra were obtained for translucent anhedral grains handpicked from lightly ground type angastonite M45575 under a binocular microscope, as well as from a different specimen from the type locality, South Australian Museum specimen G32227. Spectra were also recorded for minyulite associated with the amorphous phase in the angastonite type specimen M45575 and for penriceite growing on the amorphous phase in a specimen from the type locality. The spectra were obtained using a Nicolet 5700 FTIR spectrometer (range 4000 to 700 cm^{-1}) equipped with a Nicolet Continuum IR microscope and a diamond-anvil cell and are shown in Fig. 3.

The two different angastonite specimens have identical spectra. The angastonite phase spectra differ in detail from the spectra for crystalline minyulite and penriceite but are much closer to the latter, which crystallises and grows from the amorphous phase. The broad O-H stretch region has a peak at 3380 cm^{-1} and shoulders at 2930, 3200 and 3620 cm^{-1} . The bands in the range 2930 to 3380 cm^{-1} correspond to H-bonded O...O distances in the range 2.7 to 2.8 Å (Libowitzky, 1999), while the shoulder at 3620 cm^{-1} is most likely due to hydroxyls. The H–O–H bending mode region contains two peaks at 1560 and 1640 cm^{-1} . A weak peak at 1430 cm^{-1} may be due to carbonate impurity. The P–O stretching region has peaks at 1020, 1050 and 1090 cm^{-1} , with a shoulder at 990 cm^{-1} . The shoulder and the peak at 1020 cm^{-1} correspond to symmetric P–O stretching modes while the two higher-wavenumber peaks correspond to anti-symmetric stretching modes.

3.3 Chemical composition

The samples analysed were the angastonite type specimen M45575; a specimen from the type locality, G32227; and a

specimen from Tom's quarry, about 15 km from the Penrice quarry (Elliott et al., 2013). The Tom's quarry specimen gave no crystalline peaks in the PXRD.

The analyses of the anhedral, globular grains of angastonite in each specimen were made using wavelength-dispersive spectrometry on a JEOL JXA-8500F Hyperprobe operated at an accelerating voltage of 15 kV and a beam current of 2 nA. The amorphous angastonite was extremely beam-sensitive, and the beam was defocused to 10 μm to minimise beam damage. Analytical results are given in Table 1. The H_2O is based on Mills et al. (2008) CHN analyses. Empirical formulae, normalised to 2 P atoms, are

for M45575, $\text{Na}_{0.33}\text{K}_{0.04}\text{Ca}_{0.97}\text{Mg}_{1.08}\text{Al}_{2.00}(\text{PO}_4)_2\text{F}_{0.77}(\text{OH})_{3.75} \cdot 6.96\text{H}_2\text{O}$;

for G32227, $\text{Na}_{0.16}\text{K}_{0.01}\text{Ca}_{1.14}\text{Mg}_{1.08}\text{Al}_{1.95}(\text{PO}_4)_2\text{F}_{0.57}(\text{OH})_{3.91} \cdot 7.90\text{H}_2\text{O}$;

for Tom's Q, $\text{Na}_{0.20}\text{K}_{0.01}\text{Ca}_{1.19}\text{Mg}_{1.12}\text{Al}_{2.38}(\text{PO}_4)_2\text{F}_{0.14}(\text{OH})_{5.83} \cdot 7.34\text{H}_2\text{O}$.

The analyses are consistent across different specimens and localities, except for the extent of hydration as reflected in the variable analysis totals and some minor variability in the Al_2O_3 and P_2O_5 contents. Overall, the empirical analyses conform to the ideal formula of $\text{CaMgAl}_2(\text{PO}_4)_2(\text{OH})_4 \cdot 7\text{H}_2\text{O}$ reported by Mills et al. (2008). These authors did not analyse for Na or F, but as seen from Table 1, these are minor components that do not modify the ideal formula.

3.4 Powder X-ray diffraction

A PXRD for type angastonite is shown in Fig. 4, label a, where it is compared with almost single-phase specimens corresponding to (b) the 10 Å phase, (c) the 11 Å phase and (d) penriceite. The figure shows that the type specimen is a mixture of these three phases plus minyulite. The amorphous-phase contribution to the PXRD for type angastonite is shown in Fig. 5 by the broad humps centred at $2\theta \approx 25$ and $2\theta \approx 35$ ($\text{CoK}\alpha$). For comparison, Fig. 5 shows the PXRD for a Tom's quarry specimen, which has an analysis similar to that for type angastonite except for lower P_2O_5 and F contents. The PXRD has only broad humps characteristic of an amorphous phase. The combined PXRD results show that the type specimen of angastonite contains four crystalline phases: minyulite, penriceite, and a 10 and an 11 Å layer phase, together with an amorphous phase which is now approved as angastonite.

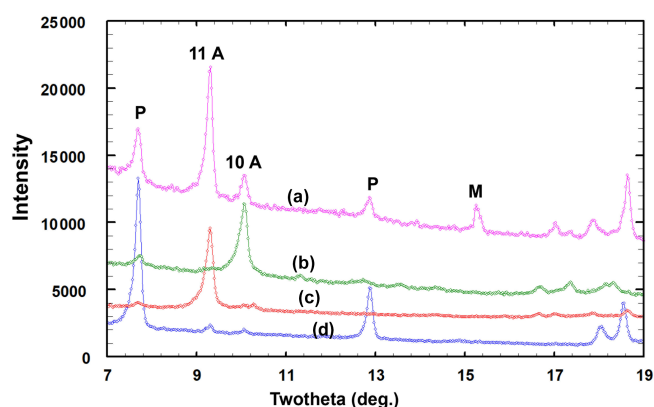
4 Discussion

Angastonite has an unusually low measured density of only 1.57(2) g cm^{-3} . For comparison the amorphous iron phosphate mineral santabarbarite, $\text{Fe}_3(\text{PO}_4)_2(\text{OH})_3 \cdot 5\text{H}_2\text{O}$ (Pratesi et al., 2003), has a measured density of 2.42 g cm^{-3} ,

Table 1. Electron microprobe analyses, standard deviations in parentheses.

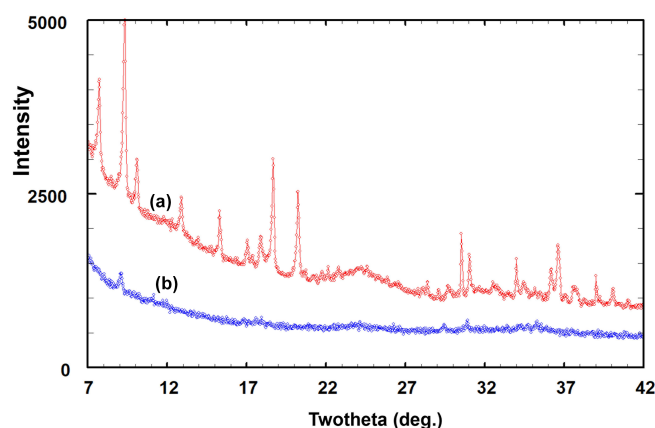
	M45575 avg. of 7	G32227 avg. of 5	Tom's quarry avg. of 4	Mills et al. (2008)	Standards
Na ₂ O	2.05 (0.38)	0.88 (0.15)	1.05 (0.09)	*n.a.	Albite
K ₂ O	0.38 (0.16)	0.07 (0.02)	0.04 (0.01)	0.09	Adularite
CaO	10.8 (2.0)	11.3 (0.9)	11.4 (1.1)	9.87	Apatite
MgO	8.62 (0.70)	7.71(0.48)	7.69 (0.66)	8.17	Spinel
Al ₂ O ₃	20.2 (1.4)	17.6 (1.1)	20.6 (1.0)	18.0	Berlinite
P ₂ O ₅	28.0 (2.0)	25.1 (1.3)	24.1 (0.9)	26.1	Berlinite
F	2.89 (0.48)	1.87 (0.21)	0.46 (0.70)	*n.a.	Fluorite
H ₂ O	31.4	31.4	31.4	31.4	
-O=F	-1.18	-0.79	-0.19		
Total	103.1	95.1	96.5	93.7	

* n.a. means not analysed.

**Figure 4.** Low-angle region of PXRD patterns (CoK α radiation) corresponding to the (a) angastonite type specimen M45575, (b) 10 Å phase, (c) 11 Å phase and (d) penriceite (P). Minor minyulite (M) is also present.

and replacing Fe with Al gives a calculated density of 2.00 g cm⁻³. Amorphous bolivarite, Al₂(PO₄)(OH)₃ · 4-5H₂O, has a measured density of 2.04 g cm⁻³, and the density of amorphous evansite, Al₃(PO₄)(OH)₆ · 6H₂O, has been reported in the range 1.8 to 2.2 g cm⁻³ (Garcia-Guinea et al., 1995). Figure 6 shows crystallisation of a crandallite-derivative mineral (the 11 Å phase) within the amorphous phase. The platy phase is accompanied by considerable microporosity which reflects the low density of the host compared to the crystalline product, for which the calculated density is 2.09 g cm⁻³.

The formula for amorphous angastonite has simple integer atomic ratios of the main constituents: Ca : Mg : Al : P is 1 : 1 : 2 : 2. These ratios are reproducible in different specimens from different localities. The simplicity and constancy of the formula suggest that although angastonite does not display long-range ordering (absence of Bragg peaks in the PXRD), it must have a high degree of local order, most likely

**Figure 5.** PXRD patterns (CoK α) of the (a) angastonite type specimen M45575 and (b) amorphous phase in the Tom's quarry specimen.

in the form of locally ordered clusters that are more or less randomly oriented relative to one another. In considering possible models for the clusters, we took into account that they would be expected to have features in common with the crandallite-type structure. This is because amorphous angastonite recrystallises internally to crandallite-derivative structures (Fig. 6) during supergene alteration at close-to-ambient conditions, so only small-scale diffusion of atoms can be involved in the process.

Figure 7 shows the structure of a possible local cluster with the composition CaMgAl₂(PO₄)₂X₁₁ (X denotes OH and H₂O). Adjusting OH and H₂O to achieve charge balance gives the formula for angastonite, CaMgAl₂(PO₄)₂(OH)₄ · 7H₂O. The cluster comprises a triangular corner-shared grouping of two Al-centred octahedra and a Mg-centred octahedron. The octahedra are tilted so that three apices are shared with the basal anions of a PO₄ group, while a second PO₄ group shares corners with the opposite apex of one of the octahedra. The Ca²⁺ cation nestles in the cavity formed

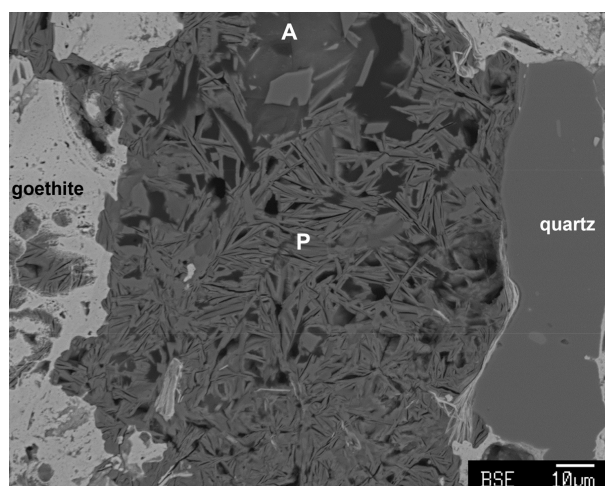


Figure 6. Sectioned type specimen M45575 showing crystallisation of amorphous angastonite (A) to platelets (P, edge-on) of the 11 Å phase. Microporosity is associated with the platelet formation.

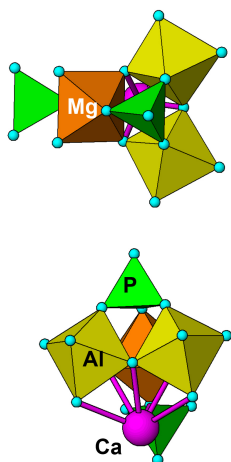


Figure 7. Two views of a cluster of composition $\text{CaMgAl}_2(\text{PO}_4)_2(\text{OH})_4 \cdot 7\text{H}_2\text{O}$, representing a possible model for local order in amorphous angastonite.

by the triad of tilted octahedra and coordinates to six anions of the cluster. It is likely that the second PO_4 group orients to provide two further anions coordinating to Ca. The pair of corner-connected Al-centred octahedra in the cluster together with the associated corner-connected PO_4 group has the same topology as that for Al-centred octahedral dimers in minyulite, from which angastonite is derived.

The cluster shown in Fig. 7 is topologically identical to a small element of the crandallite structure type. A view of the crandallite-type layer in the 11 Å phase is shown in Fig. 8 for comparison, where one of the clusters is circled. Crandallite-type layers of composition $\text{MgAl}_2(\text{PO}_4)_2(\text{OH},\text{H}_2\text{O})_6$ in angastonite can be formed by condensation of the clusters shown in Fig. 7 via octahedral corner sharing. The cluster

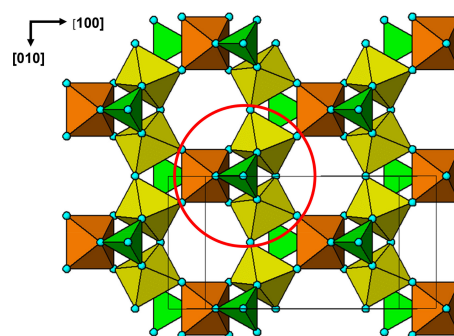


Figure 8. The (100) layer of crandallite-type structure in the 11 Å phase. The cluster corresponding to that shown in Fig. 7 is circled.

condensation probably involves rotations of adjacent clusters without large displacements.

4.1 Status of amorphous minerals

The subordinate status of amorphous minerals is evident from that fact that there has been no overview of the topic since the seminal paper by Rogers (1917) over 100 years ago. At that time, mineralogists relied on morphological and optical measurements, together with chemical analyses, to characterise minerals. Rogers noted that of the ~ 1000 distinct mineral species reported in *Dana's System of Mineralogy*, only 17 were listed as amorphous. In the ensuing decades, with progressively wider use of X-ray diffraction in mineral characterisation, most of the amorphous minerals were found to be crystalline or poorly crystalline. Only 5 of the 23 amorphous minerals studied by Rogers have been given IMA-approved status as “grandfathered”, i.e. described before the Commission on New Minerals and Mineral Names (now the CNMNC) was established in 1959. They are allopahne, evansite, opal, pitticite and stibiconite. A further 6 minerals have been approved as amorphous minerals or redefined amorphous minerals since 1959. These are given in Table 2. Nickel (1995) provided some guiding principles for distinguishing amorphous minerals by first defining the term “crystalline” as meaning having “atomic ordering on a scale that can produce an ‘indexable’ (i.e. with Miller indices) diffraction pattern when the substance is traversed by a wave with a suitable wavelength (X-ray, electrons, neutrons, etc.)”. He suggested that the requirements for accepting a naturally occurring amorphous phase as a mineral include complete quantitative chemical analyses sufficient to reveal a homogeneous chemical composition in the grains of the specimen, physicochemical (normally spectroscopic) data that prove the uniqueness of the phase, and evidence that the phase cannot produce an indexable diffraction pattern both in the natural state and after treatment by some physicochemical process (such as heating).

Since the publication of Nickel’s guidelines, only santabarbarite, $\text{Fe}_3(\text{PO}_4)_2(\text{OH})_3 \cdot 5\text{H}_2\text{O}$ (Pratesi et al.,

Table 2. IMA CNMNC-approved amorphous minerals since 1959.

Mineral	IMA-approved	Formula	Reference
Thorsteenstrupine	1962	(Ca,Th,Mn) ₃ Si ₄ O ₁₁ F·6H ₂ O	Kupriyanova et al. (1962)
Meymacite	1965	WO ₃ ·2H ₂ O	Pierrot and van Tassel (1965)
Umbozerite	1974	Na ₃ Sr ₄ Th[Si(O,OH) _{3–4}] ₈	Es'kova et al. (1974)
Calciouranoite	1974	(Ca,Ba,Pb)U ₂ O ₇ ·5H ₂ O	Rogova et al. (1974)
Georgeite	1979	Cu ₂ (CO ₃)(OH) ₂ ·6H ₂ O	Bridge and Hey (1979)
Santabarbaraite	2003	Fe ³⁺ ₃ (PO ₄) ₂ (OH) ₃ ·5H ₂ O	Pratesi et al. (2003)
Angastonite	2021	CaMgAl ₂ (PO ₄) ₂ (OH) ₄ ·7H ₂ O	This study

2003), has been approved as an amorphous mineral by the IMA CNMNC. Pratesi et al. (2003) made extensive use of X-ray absorption spectroscopy (XANES and EXAFS) to help establish the anion coordination environment of the Fe³⁺ cations. The study also confirmed a genetic relationship with vivianite, where amorphous santabarbaraite is the end product of progressive oxidation and dehydration of vivianite. Such a genetic relationship helps confirm the uniqueness of the chemical composition. A similar genetic relationship has been established between malachite and its amorphous analogue georgeite, Cu₅(CO₃)₃(OH)₄·6H₂O (Pollard et al., 1991). In the current study, the genetic relationship between amorphous angastonite and the precursor mineral minyulite, as well as between angastonite and the crandallite-derivative phases formed during crystallisation of the amorphous phase, helped to envisage a model for the local order in the amorphous phase.

The unambiguous determination of the local structure of amorphous and poorly crystalline minerals that do not have integer indexing of Bragg peaks is notoriously difficult. A procedure that has come into prominence for these types of materials involves the analysis of the Fourier transform of the total scattering data, giving the pair-distribution function (PDF) that is closely related to the radial distribution function used for analysing glasses and liquids (Billinge, 2008). The PDF gives the distribution of interatomic bond lengths, weighted by the scattering powers of the contributing atoms. Having this distribution can help eliminate potential models for the short-range structural order, but it cannot give a unique solution for the local structure. This is well evidenced by the ongoing controversy surrounding the structure of the low-crystallinity mineral ferrihydrite, where uncertainly remains concerning the structure (Manceau, 2019). Another approach used for minerals that do not have indexable Bragg peaks in the PXRD is the application of the Debye equation (Debye, 1915) for modelling the total scattering in the PXRD (Bragg plus diffuse scattering). Harrington et al. (2012) have shown how the PDF and Debye methods can be combined to maximise the information on the local structure obtainable from PXRD patterns of highly disordered materials. We have recently applied the combination of PDF and Debye methods to establish a model for the local order in amorphous

titania (Grey et al., 2021). It is possible that a high-energy synchrotron X-ray data collection on angastonite, with calculation of the PDF, could provide additional information on its local structure.

4.2 Note added after submission

Since the submission of this paper, the mineral designated as the 11 Å phase has been approved as a new mineral, eliottite with the formula NaMgAl₃(PO₄)₂F₆·9H₂O, by the IMA CNMNC (Grey et al., 2022, unpublished data).

Data availability. No data sets were used in this article.

Author contributions. IEG oversaw the research and wrote the manuscript; PE supplied the specimens; WGM assisted in the data processing; CMM conducted the microprobe analyses; ARK measured the density and refractive index; SJM provided the type specimen of angastonite.

Competing interests. The contact author has declared that neither they nor their co-authors have any competing interests.

Disclaimer. Publisher's note: Copernicus Publications remains neutral with regard to jurisdictional claims in published maps and institutional affiliations.

Acknowledgements. The authors thank Cameron Davidson and Matthew Glenn for help with electron microprobe sample preparation and SEM studies. The infrared spectrum was acquired with the assistance of the Forensic Science Centre, Adelaide. We acknowledge the Diffraction Laboratory at CSIRO Mineral Resources, Clayton, for use of their Panalytical Empyrean powder XRD diffractometer. Thanks to Dmitry Pushcharovsky and the anonymous referee for their helpful comments.

Review statement. This paper was edited by Cristiano Ferraris and reviewed by Dmitry Pushcharovsky and one anonymous referee.

References

- Billinge, S. J. L.: Nanoscale structural order from the atomic pair distribution function (PDF): there's plenty of room in the middle, *J. Solid State Chem.*, 181, 1695–1700, 2008.
- Bridge, P. J. and Hey, M.: Georgeite, a new amorphous copper carbonate from the Carr Boyd Mine, Western Australia, *Mineral. Mag.*, 43, 97–98, 1979.
- Debye, P.: Dispersion of Roentgen rays, *Ann. Phys.*, 46, 809–823, 1915.
- Elliott, P., Peisley, V., and Mills, S. J.: The phosphate deposits of South Australia, *Aust. J. Mineral.*, 17, 3–32, 2013.
- Elliott, P., Grey, I. E., and Willis A. C.: Redefinition of the formula for aldermanite, $[\text{Mg}(\text{H}_2\text{O})_6][\text{Na}(\text{H}_2\text{O})_2\text{Al}_3(\text{PO}_4)_2(\text{OH},\text{F})_6]\cdot\text{H}_2\text{O}$, and its crystal structure, *Mineral. Mag.*, 85, 348–353, 2021.
- Elliott, P., Grey, I. E., Macrae, C. M., Kampf, A. R., and Davidson, C.: Penriceite, IMA 2021-068, in: CNMNC Newsletter 64, *Eur. J. Mineral.*, 34, <https://doi.org/10.5194/ejm-34-1-2022>, 2022.
- Es'kova, E. M., Semenov, E. I., Khomyakov, A. P., Mer'kov, A. N., Lebedeva, S. I., and Dubakina, L. S.: Umbozerite – a new mineral, *Dokl. Akad. Nauk. SSSR*, 216, 169–171, 1974.
- Garcia-Guinea, J., Chagoyen, A. M., and Nickel, E. H.: A re-investigation of bolivarite and evansite, *Can. Mineral.*, 33, 59–65, 1995.
- Grey, I. E., Bordet, P., and Wilson, N. C.: Structure of the amorphous titania precursor phase of N-doped photocatalysts, *RSC Adv.*, 11, 8619–8627, 2021.
- Grey, I. E., MacRae, C. M., Elliott, P., Mills, S. J., and Downes, P. J.: Minyulite, $\text{KAl}_2\text{F}(\text{PO}_4)_2 \cdot 4\text{H}_2\text{O}$. Approval of revised formula and stability in South Australian rock phosphate deposits, *Aust. J. Mineral.*, 23, 1–7, 2022.
- Harrington, R., Reinhard, B., Neder, R. B., and Parise, J. B.: The nature of x-ray scattering from geo-nanoparticles: Practical considerations of the use of the Debye equation and the pair distribution function for structure analysis, *Chem. Geol.*, 329, 3–9, 2012.
- Haseman, J. F., Lehr, J. R., and Smith, J. P.: Mineralogical character of some iron and aluminum phosphates containing potassium and ammonium, *Soil Science Soc. Proc.*, 15, 76–84, 1950.
- Kupriyanova, I. I., Stolyarova, T. I., and Sidorenko, G. A.: A new thorium silicate – thoroostenstrupine, *Zap. Vses. Mineral. Obshch.*, 91, 325–330, 1962.
- Libowitzky, E.: Correlation of O-H stretching frequencies and O-H...O hydrogen bond lengths in minerals, *Monatsh. Chemie*, 130, 1047–1059, 1999.
- Manceau, A.: Comment on “Roles of Hydration and Magnetism on the Structure of Ferrihydrite from First Principles”, *ACS Earth Space Chem.*, 3, 1576–1580, 2019.
- Mandarino, J. A.: The Gladstone-Dale relationship: Part IV. The compatibility concept and its application, *Can. Mineral.*, 19, 441–450, 1981.
- Mills, S. J., Groat, L. A., Wilson, S. A., Birch, W. D., Whitfield, P. S., and Raudsep, M.: Angastonite, $\text{CaMgAl}_2(\text{PO}_4)_2(\text{OH})_4 \cdot 7\text{H}_2\text{O}$: a new phosphate mineral from Angaston, South Australia, *Mineral. Mag.*, 72, 1011–1020, 2008.
- Miyawaki, R., Hatert, F., Pasero, M., and Mills, S. J.: IMA Commission on New Minerals, Nomenclature and Classification (CNMNC) – Newsletter 64, *Eur. J. Mineral.*, 34, 1–6, <https://doi.org/10.5194/ejm-34-1-2022>, 2022.
- Nickel, E. H.: The definition of a mineral, *Can. Mineral.*, 33, 689–690, 1995.
- Pierrot, R. and van Tassel, R.: Nouvelle définition de la meymacite et nomenclature de “acides tungstiques” naturels, *Bull. Soc. fr. minéral. cristallogr.*, 88, 613–617, 1965.
- Pollard, A. M., Thomas, R. G., Williams, P. A., Just, J., and Bridges, P. J.: The synthesis and composition of georgeite and its reactions to form other secondary carbonates, *Mineral. Mag.*, 55, 163–166, 1991.
- Pratesi, G., Cipriani, C., and Birch, W. D.: Santabarbarite: a new amorphous mineral, *Eur. J. Mineral.*, 15, 185–192, <https://doi.org/10.1127/0935-1221/2003/0015-0185>, 2003.
- Rogers, A. F.: A review of the amorphous minerals, *J. Geol.*, 25, 515–541, 1917.
- Rogova, V. P., Belov, L. N., Kiziyarov, G. N., and Koznetsova, N. N.: Calciouranoite, a new hydroxide of uranium, *Zap. Vses. Mineral. Obshch.*, 103, 108–109, 1974.
- Tatur, A.: Fluorine in ornithogenic soils and minerals on King George Island, West Antarctica, *Polish Polar Res.*, 8, 65–74, 1987.